EXTENSION OF GATO
— AN IDEAL MHD STABILITY CODE FOR AXISYMMETRIC PLASMA EQUILIBRIA TO BALLOONING MODE VARIABLES VALID FOR HIGHER (n > 5) TOROIDAL MODE NUMBERS

M.S. CHU, S.K. WONG, L.L. LAO,
A.D. TURNBULL and M.S. CHANCE*

General Atomics

APS/DPP 41st Annual Meeting
November 15–19, 1999
Seattle, Washington

****Princeton Plasma Physics Laboratory***

Abstract Submitted
for the DPP99 Meeting of
The American Physical Society

Sorting Category: 5.10 (Theoretical)

Stability of Finite-n Global Magnetohydrodynamic Modes Using the GATO Stability Code[1] M.S. CHU, S.K. WONG, L.L. LAO, A.D. TURNBULL, General Atomics, M.S. CHANCE, Princeton Plasma Physics Laboratory — This work extends the capability of the GATO stability code[2] to analyze realistic numerical tokamak equilibria for their stability to higher n ($\sim$ 5–10) MHD modes. This is motivated by the experimental evidence of these modes being relevant for both plasma termination and the behavior of ELMs. The ballooning angle transformation[3] is applied to the displacement variables in the GATO representation. The potential energy matrix is constructed with the inclusion of extra mapping quantities. The vacuum energy computed from the Greens function is also modified to couple to the transformed displacement at the plasma boundary. The resultant eigenvalue problem is solved with the modified boundary condition in the poloidal direction suitable for these transformed variables. The dependence of the plasma stability as a function of toroidal mode number and plasma equilibrium properties will be presented.

[1]Supported by U.S. DOE Grant DE-FG03-95ER54309 and Contract DE-AC02-76CH03073.
[2]L.C.Bernard *et al.*, Comput. Phys. Commun. **24**, 377 (1981).
[3]R. Gruber *et al.*, Comput. Phys. Commun. **24**, 363 (1981).

M.S. Chu
chum@fusion.gat.com
General Atomics

- [ ] Prefer Oral Session
- [X] Prefer Poster Session

Special instructions: immediately before SK Wong

Date printed: July 15, 1999

Electronic form version 1.4

OUTLINE

1. Motivation

2. Formulation

3. Implementation

4. Results

    a. Circular tokamak

    b. D-shaped cross-section

5. Summary and Results

329-99-1A

MOTIVATION

- Higher (n ~ 5) toroidal mode number MHD modes have been reported to be relevant for a number of experimental fluctuations, especially in NCS discharge at the plasma edge and also for low aspect ratio ST

- Success of correlation of these observations with either ballooning or peeling mode criterion demands a more realistic evaluation of stability of plasma to higher (n > 5)

- More intrinsic interest in the understanding of plasma behavior for higher n and non-circular cross-section especially the edge region of tokamaks with high triangularity and squareness

- The number of matrix elements required scales as $n_\psi n_\chi^2$. Computer time scales as $n_\psi n_\chi^2 \ln n_\chi$. For a tokamak configuration, $n_\psi \sim nq$ and $n_\chi \sim nq$. Therefore the computer time scales as $n^3 q^3 \ln(nq)$. An alternative formulation using the ballooning variables* allows $n_\chi \approx \text{constant}$. Therefore the resultant computer time scales as nq.

*R. Gruber et al., Computer Physics Communications 24, p. 363–376 (1981)

GATO POTENTIAL ENERGY FUNCTIONAL

$$W_p = \frac{\pi}{2}\mu_0 \int d\psi\, d\chi\, \delta W_\ell$$

where the local potential energy density δW_l is a sum of positive contributions and one negative term

$$\delta W_\ell = (\delta B_\psi)^2$$

$$+\left(\delta B_\chi + \xi_\psi J_\varphi\right)^2$$

$$+\left(\delta B_\varphi + \xi_\psi J_\chi\right)^2$$

+ Compressional Energy

$-2JX^2K$ Instability Drive

$(\vec{B}\cdot\vec{\nabla})$ TERMS IN POTENTIAL ENERGY FUNCTIONAL* FORCE THE DISPLACEMENTS (X,U,Y) TO VARY FAST IN THE POLOIDAL DIRECTION AS n INCREASES

$$W_p = \frac{\pi}{2\mu_0}\int d\psi\, d\chi\, \delta W_\ell$$

$$\begin{aligned}
\delta W_\ell = {} & \frac{1}{JB_p^2 r^2}\left|\frac{\partial X}{\partial \chi} + \frac{inJf}{r^2}X\right|^2 \\
& + JB_p^2\left| inU - \frac{\partial X}{\partial \psi} + \frac{\mu_0 j_\phi X}{rB_p^2} - \alpha\underline{\left(\frac{\partial X}{\partial \chi} + in\frac{Jf}{r^2}X\right)}\right|^2 \\
& + \frac{r^2}{J}\left| f\frac{\partial}{\partial \psi}\left(\frac{J}{r^2}\right)X + \frac{Jf}{r^2}\frac{\partial X}{\partial \psi} + \frac{\partial U}{\partial \chi}\right|^2 \\
& + \frac{\Gamma\mu_0 p}{J}\left| J\frac{\partial X}{\partial \psi} + \frac{\partial J}{\partial \psi}X + \left(\frac{\partial Y}{\partial \chi} + in\frac{Jf}{r^2}Y\right)\right. \\
& \qquad \left. + \frac{\partial}{\partial \chi}\left(\frac{r^2}{f}\right)U + \frac{r^2}{f}\frac{\partial U}{\partial \chi}\right|^2 \\
& - 2JX^2\left[\frac{\mu_0^2 j_\phi^2}{r^2 B_\phi^2} - \frac{\mu_0 j_\phi}{r}\frac{\partial}{\partial \psi}\left(\ln rB_p\right)_v - \mu_0\frac{\partial p}{\partial \psi}\frac{\partial}{\partial \psi}(\ln r)_v\right]
\end{aligned}$$

where

$$X = \vec{\xi}\cdot\vec{\nabla}\psi \;, \quad Y = \frac{r}{f}\xi_\phi \;, \quad U = \frac{f}{r^2}\left(\vec{\xi}\cdot\hat{t} - Y + J\alpha X\right)$$

Bernard, Helton, Moore, CPC <u>24</u>, p. 377 (1981).

329-99-3A

IN BALLOONING (HIGH n) VARIABLES, THE PLASMA DISPLACEMENT IS ASSUMED TO VARY SLOWLY ALONG THE FIELD LINE

Or the variation along the eikonal (toroidal) angle

$$\tilde{\phi} = \phi - \int^{\chi} \frac{fJ}{r^2} d\chi = \phi - I_q(\chi, \psi)$$

is small. The displacement is assumed to have the following dependence on this angle

$$\xi e^{in\phi} = \tilde{\xi} e^{in\tilde{\phi}} \quad .$$

Terms in the potential energy transforms in the following way

$$\frac{\partial \xi}{\partial \psi} \rightarrow \frac{\partial \tilde{\xi}}{\partial \psi} - in\tilde{\xi} I_{q,\psi}$$

$$\frac{\partial \xi}{\partial \chi} \rightarrow \frac{\partial \tilde{\xi}}{\partial \chi} - in\tilde{\xi}\frac{fJ}{r^2} \qquad \text{or}$$

$$\frac{\partial \xi}{\partial \chi} + in\frac{fJ}{r^2}\xi \rightarrow \frac{\partial \tilde{\xi}}{\partial \chi}$$

Then the potential energy functional does not contain factors of $\left[(\partial / \partial\chi) + in(Jf / r^2)\right]$ operating on physical quantities

FOR GATO POTENTIAL ENERGY FUNCTIONAL IN HIGH n VARIABLES, TERMS MULTIPLIED WITH n ARE ALWAYS IN THE COMBINATION $(U + XI_{q,\psi})$

$$\delta W_\ell = \frac{1}{JB_p^2 r^2}\left|\frac{\partial \tilde{X}}{\partial \chi}\right|^2$$

$$+ JB_p^2 \left| \underline{in\left(\tilde{U} + \tilde{X} I_{q,\psi}\right)} - \frac{\partial \tilde{X}}{\partial \psi} + \frac{\mu_0 j_\phi \tilde{X}}{rB_p^2} - \alpha \frac{\partial \tilde{X}}{\partial \chi}\right|^2$$

$$+ \frac{r^2}{J}\left| - in\frac{fJ}{r^2}\left(\tilde{U} + \tilde{X} I_{q,\psi}\right) + \frac{\partial \tilde{U}}{\partial \chi} + \frac{Jf}{r^2}\frac{\partial \tilde{X}}{\partial \psi} + f\frac{\partial}{\partial \psi}\left(\frac{J}{r^2}\right)\tilde{X}\right|^2$$

$$+ \frac{\Gamma \mu_0 p}{J}\left| \underline{inJ\left(\tilde{U} + \tilde{X} I_{q,\psi}\right)} + J\frac{\partial \tilde{X}}{\partial \psi} + \frac{\partial J}{\partial \psi}\tilde{X}\right.$$

$$\left. + \frac{\partial \tilde{Y}}{\partial \chi} + \frac{\partial}{\partial \chi}\left(\frac{r^2}{f}\right)\tilde{U} + \frac{r^2}{f}\frac{\partial \tilde{U}}{\partial \chi}\right|$$

$$- 2JX^2K$$

329-99-4A

BOUNDARY CONDITION

With the ballooning angle transformation, the computation domain remains

$$\chi_0 \le \chi \le \chi_0 + 2\pi$$

But the boundary condition is changed from

$$\xi(\chi_0 + 2\pi) = \xi(\chi_0)$$

to

$$\tilde{\xi}(\chi_0 + 2\pi) = \tilde{\xi}(\chi_0)\, e^{2inq(\psi)\pi}$$

VACUUM ENERGY

The vacuum package has to be modified to accept the $\tilde{\xi}$ as input variable

$$\delta W_v = \sum_{i,j} X_i w_{ij}^{vac} X_j$$

transforms into

$$W_v = \sum_{i,j} \tilde{X}_i \tilde{w}_{ij}^{vac} \tilde{X}_j$$

where

$$\tilde{w}_{ij}^{vac} = e^{in[q(\chi_i) - q(\chi_j)]} w_{ij}^{vac}$$

For high n, accurate vacuum energy computation requires putting more grid points at the vacuum boundary than inner plasma surfaces

MODIFICATIONS TO THE GATO CODE PACKAGE

(1) Mapping: Compute $I_q(\chi, \psi)$, $I_{q,\psi}$

(2) Matrix Elements Generation:

Compute δW_l, δW_v

(3) Eigenvalue Solver: No change

(4) Plotting: transform back from $\tilde{\xi}$ to ξ

COMPARISON OF n = 10 MODE FOURIER HARMONICS OF (ξ_ψ, ξ_χ)

With ballooning transformation only low order harmonics are large

Fourier Analysis for imag Xpsi, chi = pest chi

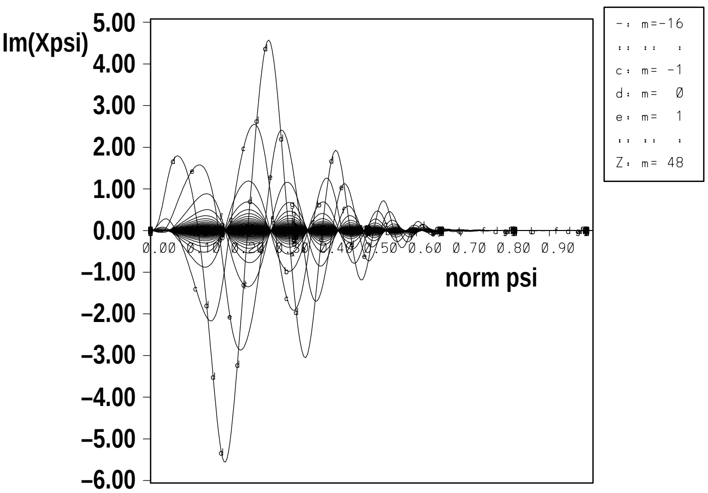

Fourier Analysis for real Xchi : chi = pest chi

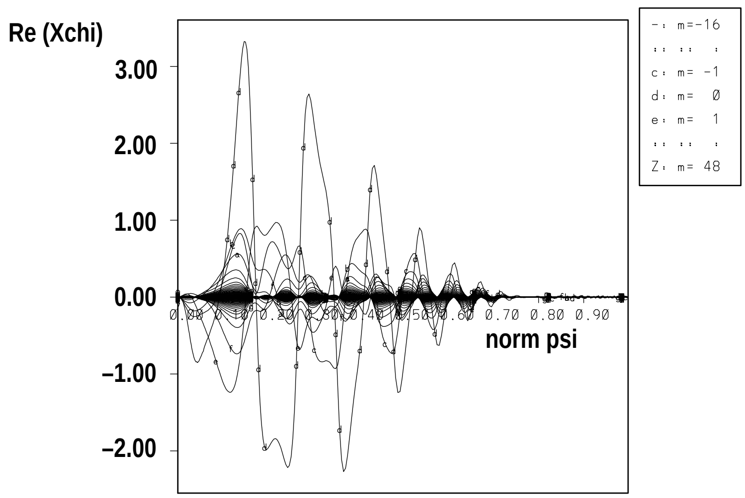

Without ballooning transformation higher order harmonics present

Fourier Analysis for imag Xpsi, chi = pest chi

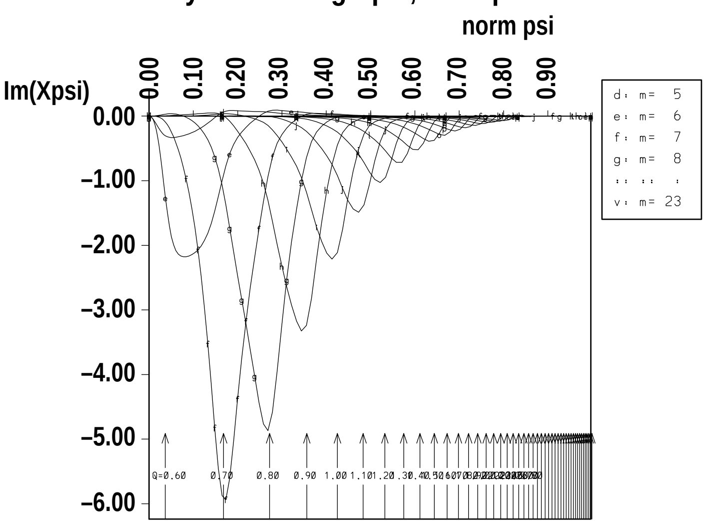

Fourier Analysis for real Xchi : chi = pest chi

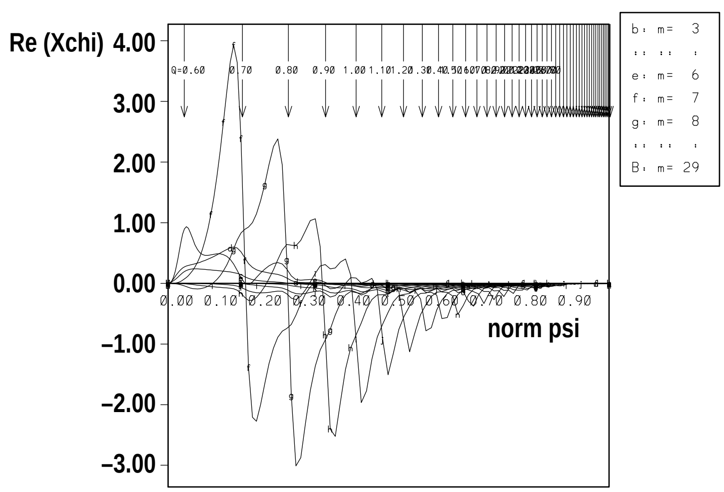

COMPARISON OF GROWTH RATES

- For the equilibrium with a circular cross-section the growth rate using ballooning transformation converges relatively fast at high n. Shown are the comparison of growth rates as a function number of flux surfaces and grid points ($n_\psi \times n_\chi$).

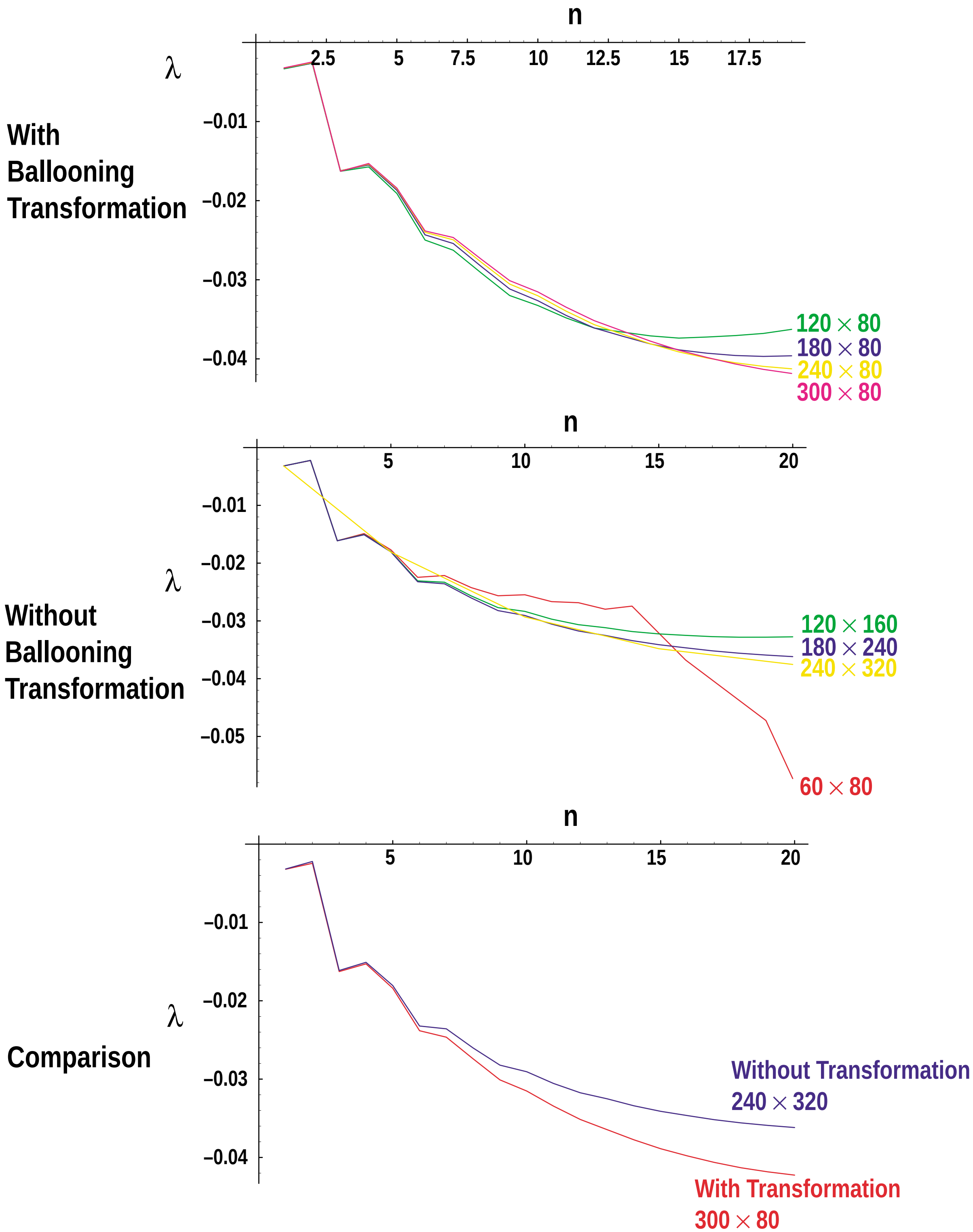

329-99-12 jy

COMPARISON OF n = 5 MODE (X)

With ballooning transformation

Rayleigh quotient = -0.8027E-01 *** Eigenvalue = -0.8027E-01 *** Error = 0.5605E-06
Maximum number of iterations = 35 *** 8 Inverse iterations done
There are 0 eigenvalues less than -0.8027E-01 *** nevp = 2
ntor = 5 jpsi = 300 itht = 80 rext = 1.000 qaxe = 0.80695 phi = 0.00000pi

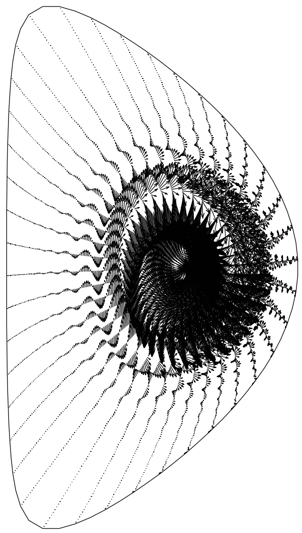

Displacement psi vs. Psi at chi (1) = 0.01250pi

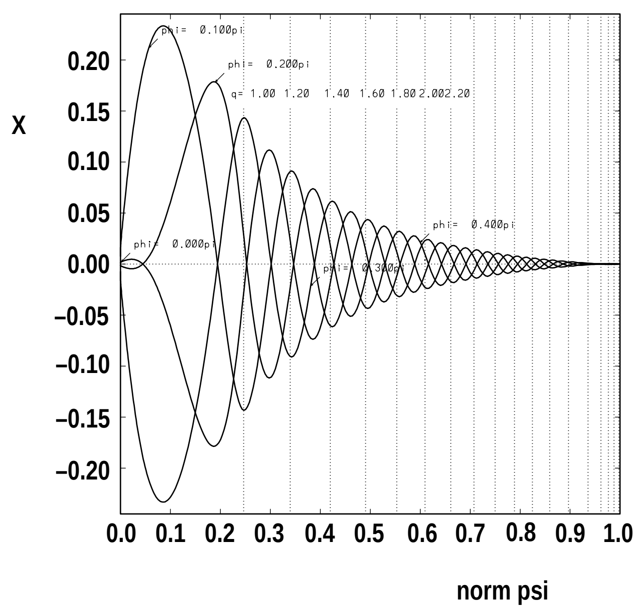

Without ballooning transformation

Rayleigh quotient = -0.7731E-01 *** Eigenvalue = -0.7731E-01 *** Error = 0.7951E-05
Maximum number of iterations = 35 *** 4 Inverse iterations done
There are 0 eigenvalues less than -0.7731E-01 *** nevp = 1
ntor = 5 jpsi = 120 itht = 240 rext = 1.000 qaxe = 0.80695 phi = 0.00000pi

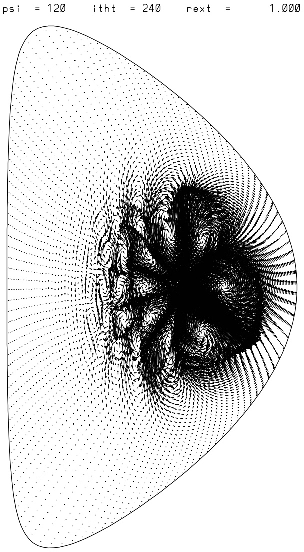

Displacement psi vs. Psi at chi (1) = 0.00417pi

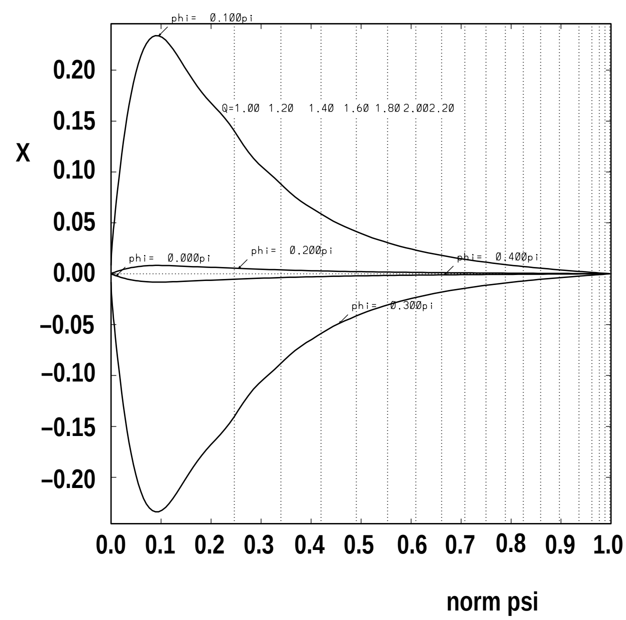

COMPARISON OF n = 10 MODE
FOURIER HARMONICS OF (ξ_ψ, ξ_χ)

With ballooning transformation
only low order harmonics are large

Fourier Analysis for imag Xpsi, chi = pest chi

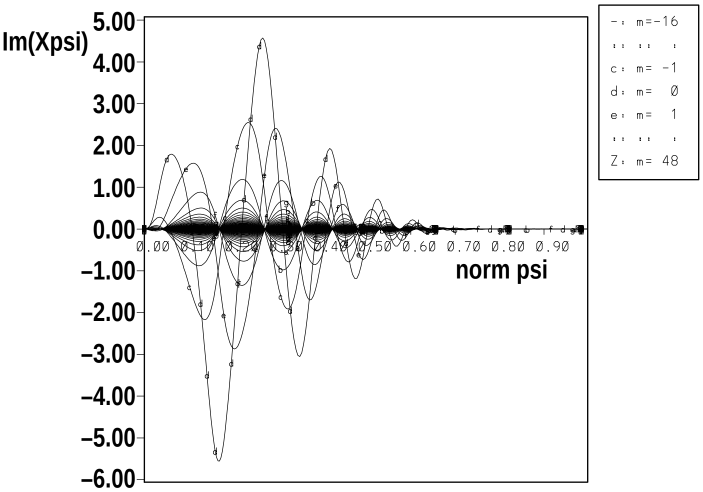

Fourier Analysis for real Xchi : chi = pest chi

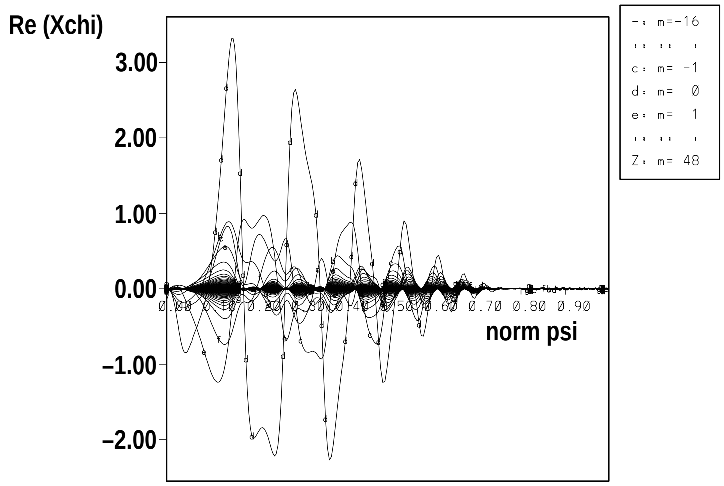

Without ballooning transformation
higher order harmonics present

Fourier Analysis for imag Xpsi, chi = pest chi

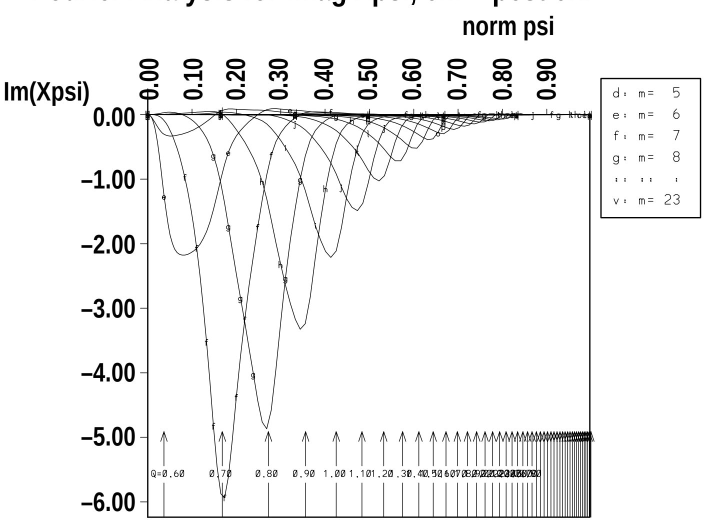

Fourier Analysis for real Xchi : chi = pest chi

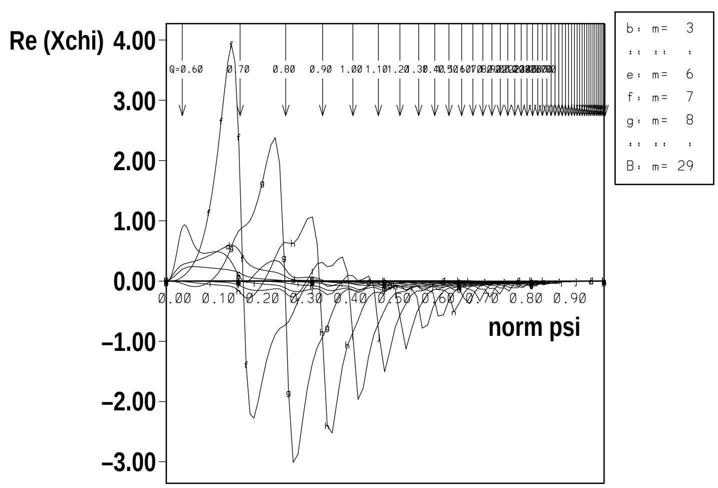

329-99-15 jy

COMPARISON OF n = 15 MODE (X)

Structure similar to low n

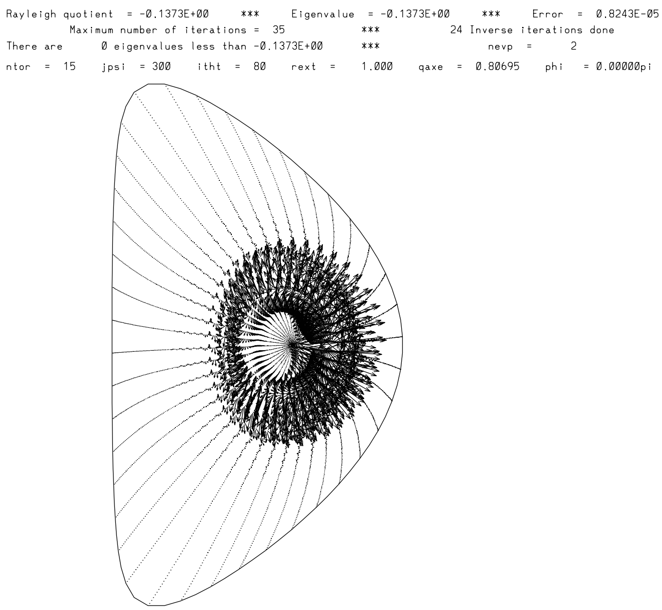

Lower harmonics

Fourier Analysis for imag Xpsi: chi = pest chi

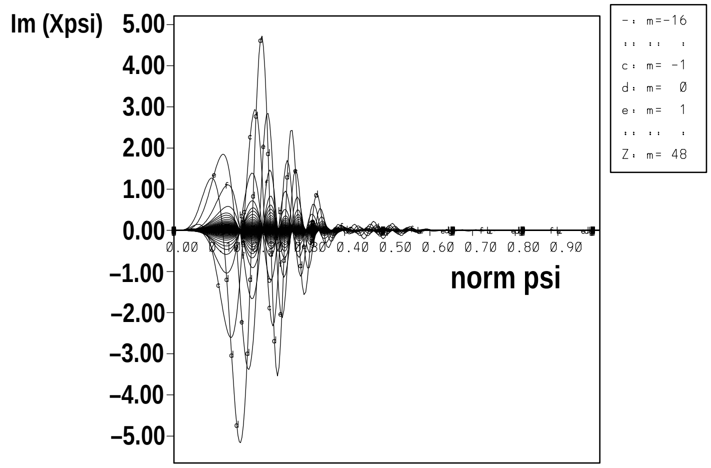

Finger like structure

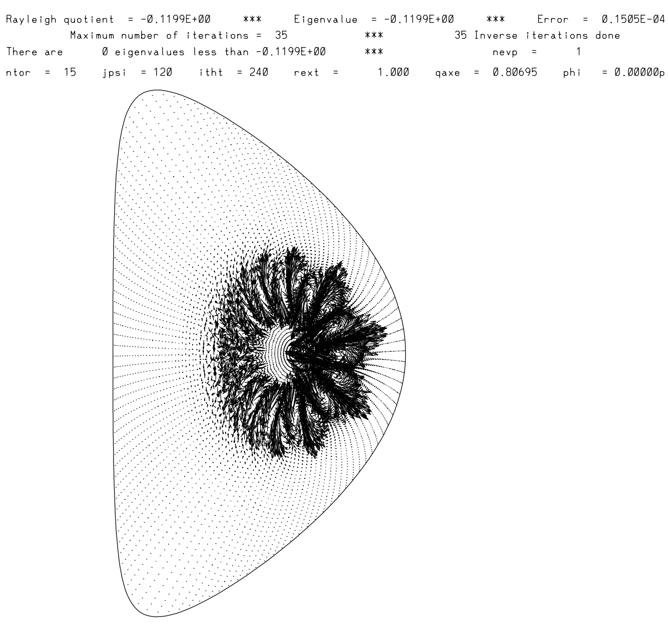

Higher harmonics

Fourier Analysis for imag Xpsi: chi = pest chi

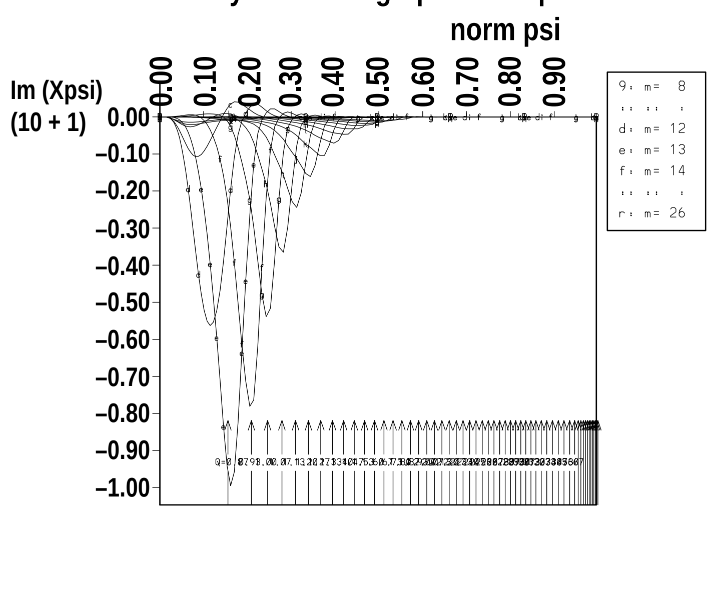

329-99-16 jy

SUMMARY AND FUTURE DIRECTIONS

(1) The GATO code has been modified to the ballooning variable

(2) Initial testing utilizing both a circular and an elongated equilibrium in DIII–D geometry indicates that this approach can be utilized to facilitate study of high (~20) n stability with modest number of grid points

(3) The vacuum package needs to be modified to the ballooning variables for the study of peeling modes (with Chance)

(4) Add an up–down symmetric option

TEST CASE: A HIGH β TOKAMAK WITH A D SHAPE CROSS–SECTION AND q_0 < 1

```
ntor    =      1
ncase   =      0
norm    =      0
nmod    =      0
nlt     =      0
nlim    =      0
jpsi    =     60
itht    =     80
isym    =      0
nmap    =      1
igrid   =      0
idnsty  =      0
nham1   =      0
nham2   =      0
nham3   =      2
nmesh   =      2
peqpk0  =  0.50000000E+00
peqpk1  =  0.50000000E+00
peqpk2  =  0.50000000E+00
psipak  =  0.20000000E+01
psincr  =  0.99500000E+00
chiwth  =  0.00000000E+00
dpsisl  =  0.00000000E+00
epsaxs  =  0.10000000E-06
stepfac =  0.20000000E-01
flxstp  =  0.15000000E+00
delac   =  0.10000000E-01
psispl  =  0.10000000E-01
errsep  =  0.30000000E-04
delpakf =  0.00000000E+00
delpakc =  0.00000000E+00
delpkf  =  0.15000000E+00
delpkc  =  0.10000000E-01
psichek =  0.10000000E-07
boxtnd  =  0.10000000E+00
qptol   =  0.10000000E-01
bperor  =  0.50000000E-01
sersnm  =  0.10000000E-08
sertnm  =  0.10000000E-07
arcmin  =  0.20000000E-02
delgap  =  0.10000000E+00
stepcut =  0.50000000E+00
endtol  =  0.10000000E+00
cnvmag  =  0.10000000E-09
nwtmag  =     25
npfit   =    150
numstp  =      5
npcmin  =      1
narcln  =    120
nangax  =    144
nanglm  =    360
narcmx  =    721
nbpmax  =      5
nwtmax  =     20
nslmax  =     10
nhfmax  =      4
ntrymx  =      1
ntdecr  =      7
ntmmin  =    360
tolspln =  0.25000000E+00
roundff =  0.10000000E-10
bigno   =  0.10000000E+31
ibal    =      1
```

gato–DIII–D
gato–DIII–D
n = 1 Wall at 1.00∗a

```
btdes   =  0.00000000E+00
qxin    =  0.00000000E+00
qsurf   =  0.20000000E+01
gamma   =  0.16666667E+01
rmantl  =  0.20000000E-01
iwal    =      0
nwall   =     60
irext   =      0
rext    =  0.10000000E+01
nev     =      1
nreslv  =      0
nbrmax  =     10
nismax  =      4
ncymax  =      2
nitmax  =     35
ncyfin  =      1
al0     = -0.10000000E+01
dal0    =  0.10000000E+02
al0bas  =  0.00000000E+00
al0min  = -0.40000000E+03
al0max  = -0.10000000E-07
epschy  =  0.10000000E-04
epscon  =  0.10000000E-04
```

```
njplot  =    100
niplot  =      1
nskpi   =      2
nskpj   =      2
ncont   =     10
ncplot  =     10
ncphip  =      1
nxisgn  =      1
nxiplt  =      0
mshpsi  =      1
mshchi  =      3
nvfft   =      0
disfac  =  0.10000000E+00
scdflt  =  0.40000000E+00
iowalp  =      0
ioeqlp  =     -2
ioeigp  =      0
iopsip  =     -2
iolinp  =      0
iofftp  =      0
ioconp  =     -2
iodlwp  =      0
iplotm  =      8
ioutm   =      0
ioutw   =      0
ioute   =      0
ioutp   =      9
```

```
npak    =      0
nedge   =      1
npkmax  =    370
nrat    =     15
nrepeat =      0
ncutedg =      0
cspak   =  0.50000000E+00
pkfrac  =  0.66666667E+00
qpfrac  =  0.33333333E+00
sedg0   =  0.00000000E+00
sedg1   =  0.00000000E+00
epsrat  =  0.10000000E-09
minpak  =      1
maxpak  =      4
incpak  =      4
epspak  =  0.10000000E-01
spakmn  =  0.10000000E+00
swidmn  =  0.10000000E+01
swidmx  =  0.10000000E+03
```

Equilibrium Grid
Equal Arc coordinates

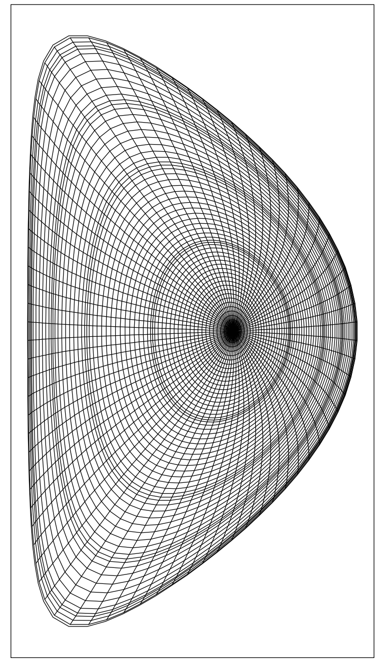

version: vs 09/95

jpsi	60	rcnt	1.70000E+00	qcyl	1.12640E+00
itht	80	rcgeom	1.69950E+00	q0surf	0.00000E+00
nmap	1	aminor	6.49482E-01	volume	0.00000E+00
ncase	0	epslon	3.82161E-01	vhalf	0.00000E+00
isym	0	capa	1.80486E+00	welln	0.00000E+00
redge	9.85000E-01	triangl	6.95466E-01	bpave	0.00000E+00
xdim	1.43000E+00	xaxis	1.85923E+00	btave	0.00000E+00
zdim	2.57378E+00	eaxe	1.33880E+00	betap	0.00000E+00
psilim	3.20000E-01	taxe	0.00000E+00	betat	0.00000E+00
psisep	0.00000E+00	qaxe	8.06948E-01	bpornl	0.00000E+00
psimaxu	0.00000E+00	qmer	0.00000E+00	allim	0.00000E+00
psimaxl	0.00000E+00	btmer	0.00000E+00	mantle	0.00000E+00
btor	1.52299E+00				
totcur	1.67798E+06				

Plot of q and n vs psi

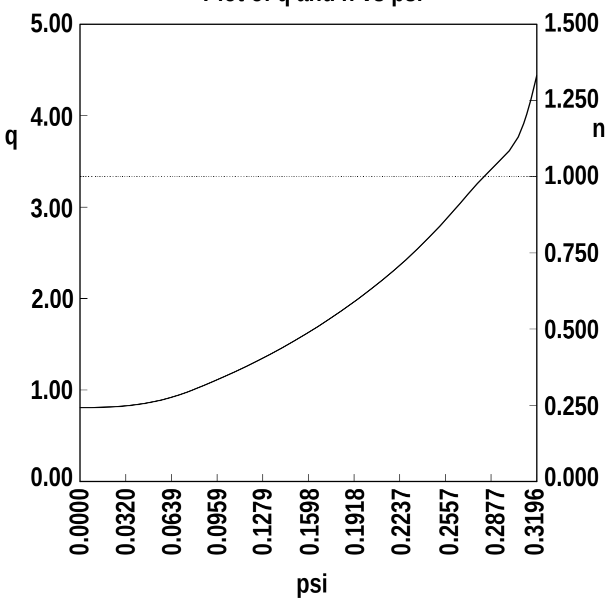

329-99 jy

COMPARISON OF GROWTH RATES

- For the equilibrium with DIII–D cross-section the growth rate using ballooning transformation converges relatively fast at high n. Shown are the comparison of growth rates as a function of number of flux surfaces and grid points in the poloidal direction ($n_\psi \times n_\chi$).

With Ballooning Transformation

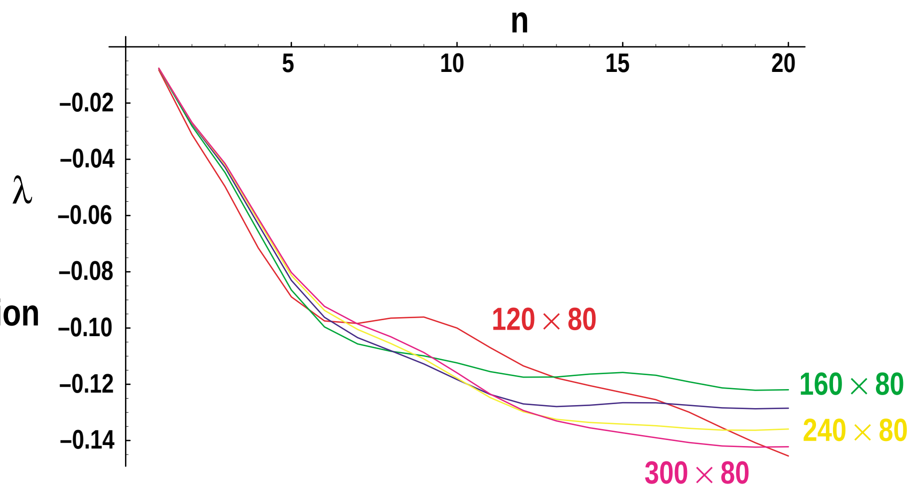

Without Ballooning Transformation

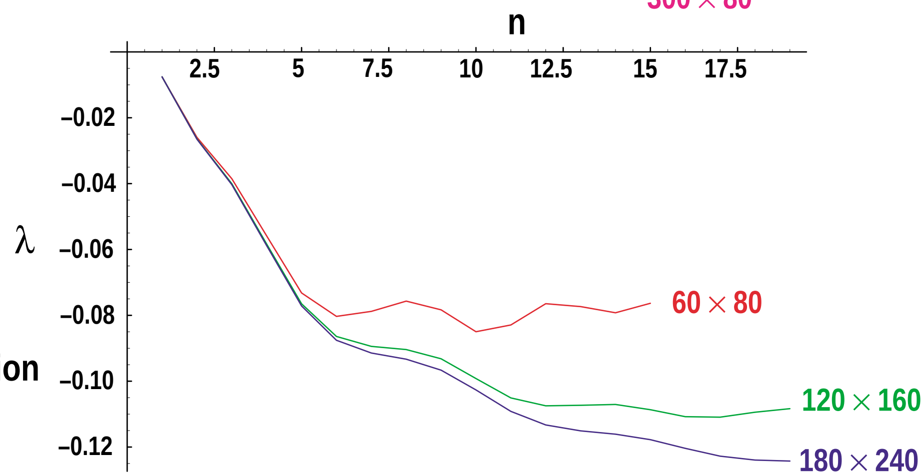

Comparison

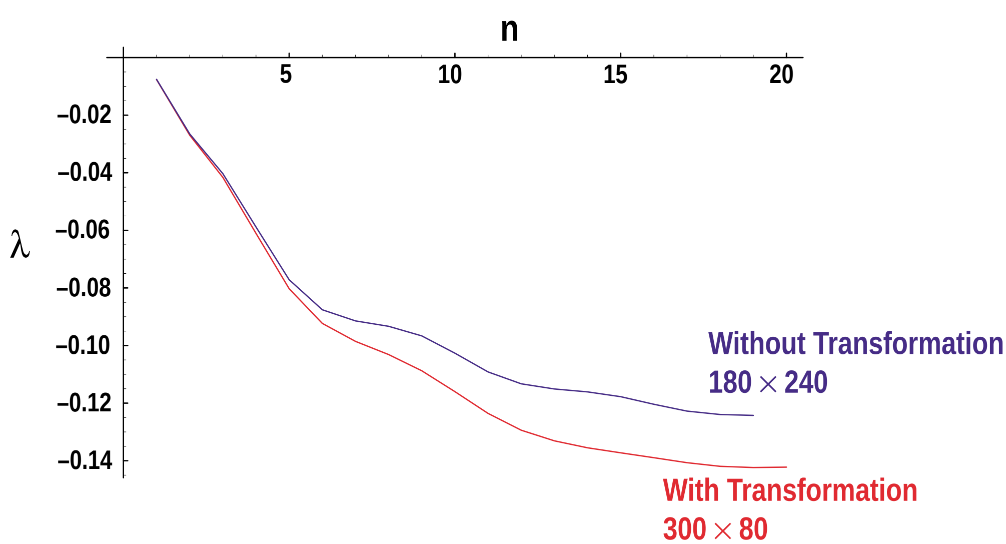

329-99 jy

COMPARISON OF n = 5 MODE (X)

With ballooning transformation

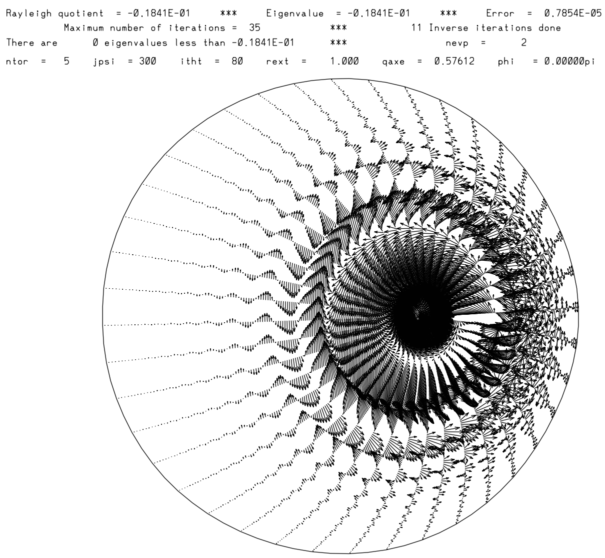

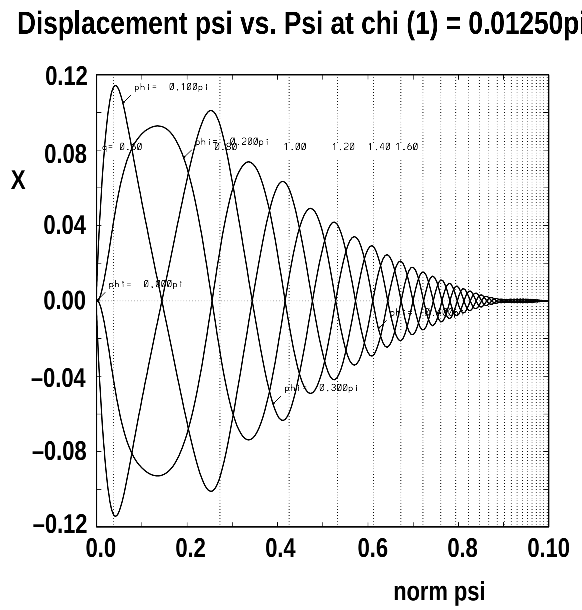

Without ballooning transformation

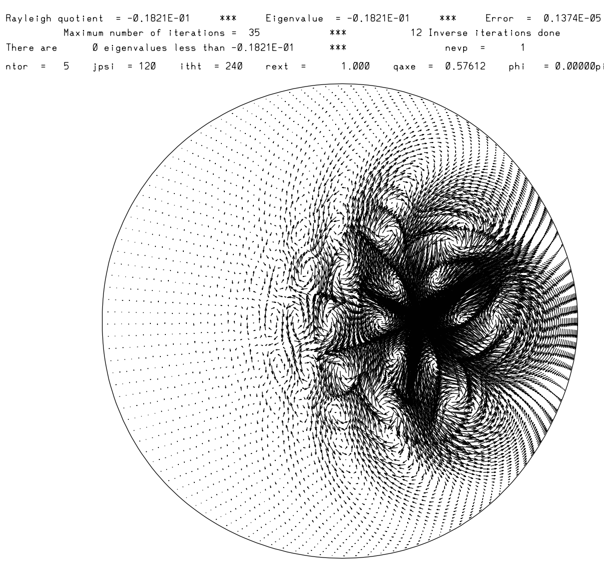

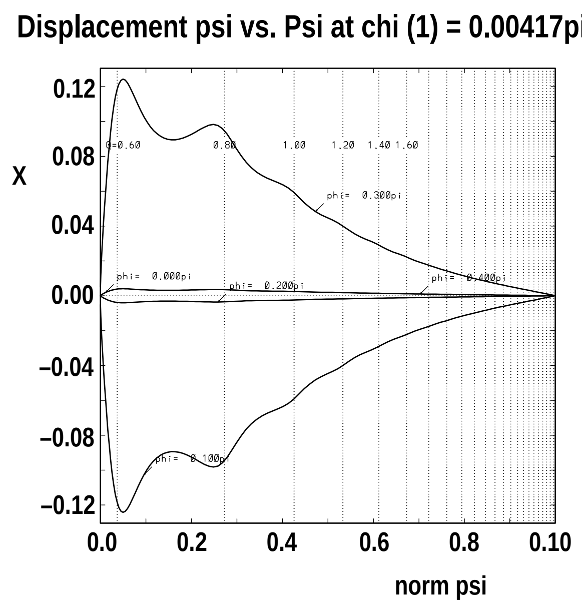

329-99 jy

TEST CASE: A HIGH β TOKAMAK WITH A CIRCULAR CROSS-SECTION AND $q_0 < 1$

```
ntor    =     1
ncase   =     0
norm    =     0
nmod    =     0
nlt     =     0
nlim    =     0
jpsi    =    60
itht    =    80
isym    =     0
nmap    =     1
igrid   =     0
idnsty  =     0
nham1   =     0
nham2   =     0
nham3   =     2
nmesh   =     2
peqpk0  =  0.50000000E+00
peqpk1  =  0.50000000E+00
peqpk2  =  0.50000000E+00
psipak  =  0.20000000E+01
psincr  =  0.99500000E+00
chiwth  =  0.00000000E+00
dpsisl  =  0.00000000E+00
epsaxs  =  0.10000000E-06
stepfac =  0.20000000E-01
flxstp  =  0.15000000E+00
delac   =  0.10000000E-01
psispl  =  0.10000000E-01
errsep  =  0.30000000E-04
delpakf =  0.00000000E+00
delpakc =  0.00000000E+00
delpkf  =  0.15000000E+00
delpkc  =  0.10000000E-01
psichek =  0.10000000E-07
boxtnd  =  0.10000000E+00
qptol   =  0.10000000E-01
bperor  =  0.50000000E-01
sersnm  =  0.10000000E-08
sertnm  =  0.10000000E-07
arcmin  =  0.20000000E-02
delgap  =  0.10000000E+00
stepcut =  0.50000000E+00
endtol  =  0.10000000E+00
cnvmag  =  0.10000000E-09
nwtmag  =    25
npfit   =   150
numstp  =     5
npcmin  =     1
narcln  =   120
nangax  =   144
nanglm  =   360
narcmx  =   721
nbpmax  =     5
nwtmax  =    20
nslmax  =    10
nhfmax  =     4
ntrymx  =     1
ntdecr  =     7
ntmmin  =   360
tolspln =  0.25000000E+00
roundff =  0.10000000E-10
bigno   =  0.10000000E+31
ibal    =     1
```

gato–circle
gato–circle
n = 1 Wall at 1.00∗a

```
btdes   =  0.00000000E+00
qxin    =  0.00000000E+00
qsurf   =  0.20000000E+01
gamma   =  0.16666667E+01
rmantl  =  0.20000000E-01
iwal    =     0
nwall   =    60
irext   =     0
rext    =  0.10000000E+01
nev     =     1
nreslv  =     0
nbrmax  =    10
nismax  =     4
ncymax  =     2
nitmax  =    35
ncyfin  =     1
al0     = -0.10000000E+01
dal0    =  0.10000000E+02
al0bas  =  0.00000000E+00
al0min  = -0.40000000E+03
al0max  = -0.10000000E-07
epschy  =  0.10000000E-04
epscon  =  0.10000000E-04
```

```
njplot  =   100
niplot  =     1
nskpi   =     2
nskpj   =     2
ncont   =    10
ncplot  =    10
ncphip  =     1
nxisgn  =     1
nxiplt  =     0
mshpsi  =     1
mshchi  =     3
nvfft   =     0
disfac  =  0.10000000E+00
scdflt  =  0.40000000E+00
iowalp  =     0
ioeqlp  =    -2
ioeigp  =     0
iopsip  =    -2
iolinp  =     0
iofftp  =     0
ioconp  =    -2
iodlwp  =     0
iplotm  =     8
ioutm   =     0
ioutw   =     0
ioute   =     0
ioutp   =     9
```

```
npak    =     0
nedge   =     1
npkmax  =   370
nrat    =    15
nrepeat =     0
ncutedg =     0
cspak   =  0.50000000E+00
pkfrac  =  0.66666667E+00
qpfrac  =  0.33333333E+00
sedg0   =  0.00000000E+00
sedg1   =  0.00000000E+00
epsrat  =  0.10000000E-09
minpak  =     1
maxpak  =     4
incpak  =     4
epspak  =  0.10000000E-01
spakmn  =  0.10000000E+00
swidmn  =  0.10000000E+01
swidmx  =  0.10000000E+03
```

Equilibrium Grid
Equal Arc Coordinates

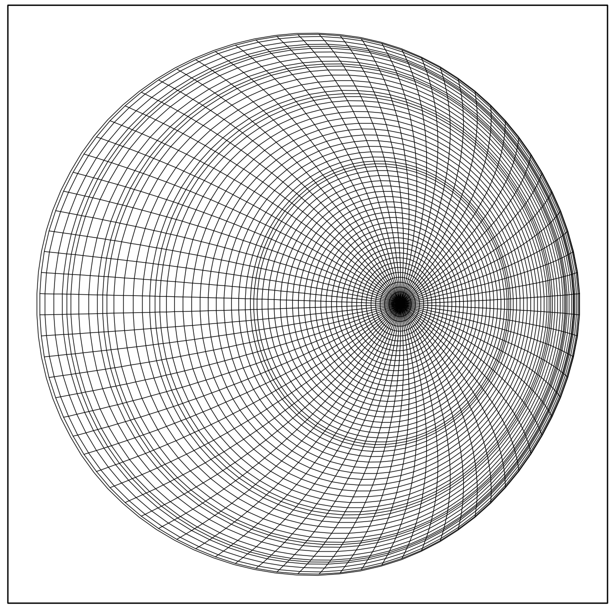

version: vs 09/95

jpsi	60
itht	80
nmap	1
ncase	0
isym	0
redge	9.55553E-01
xdim	1.36720E+00
zdim	1.36261E+00
psilim	1.68000E-01
psisep	-9.82323E-02
psimaxu	-9.82323E-02
psimaxl	0.00000E+00
btor	2.06889E+00
totcur	8.00062E+05

rcnt	1.63915E+00
rcgeom	1.63904E+00
aminor	6.20975E-01
epslon	3.78865E-01
capa	9.97535E-01
triangl	-1.14510E-02
xaxis	1.85023E+00
eaxe	1.11984E+00
taxe	0.00000E+00
qaxe	5.76124E-01
qmer	0.00000E+00
btmer	0.00000E+00

qcyl	3.04189E+00
q0surf	0.00000E+00
volume	0.00000E+00
vhalf	0.00000E+00
welln	0.00000E+00
bpave	0.00000E+00
btave	0.00000E+00
betap	0.00000E+00
betat	0.00000E+00
bpornl	0.00000E+00
allim	0.00000E+00
mantle	0.00000E+00

Plot of q and n vs psi

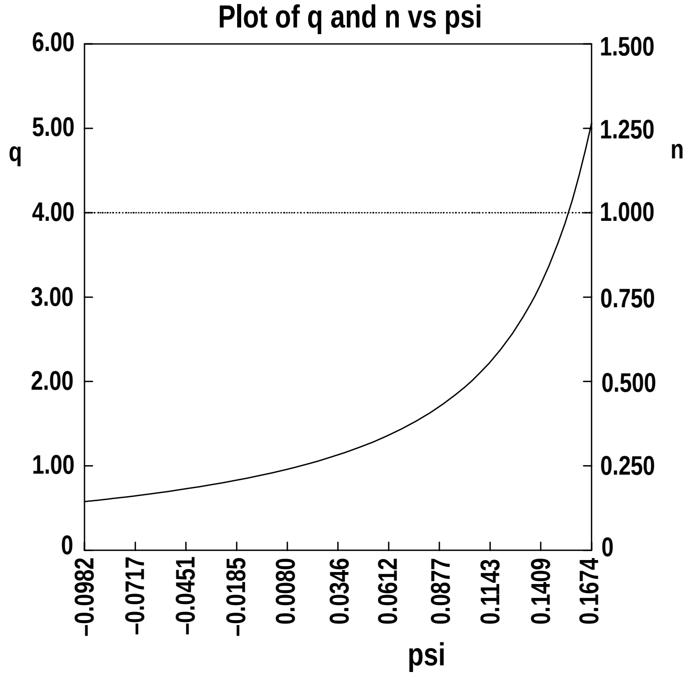

329-99 jy

COMPARISON OF n = 15 MODE (X)

With ballooning transformation

Structure similar to low n

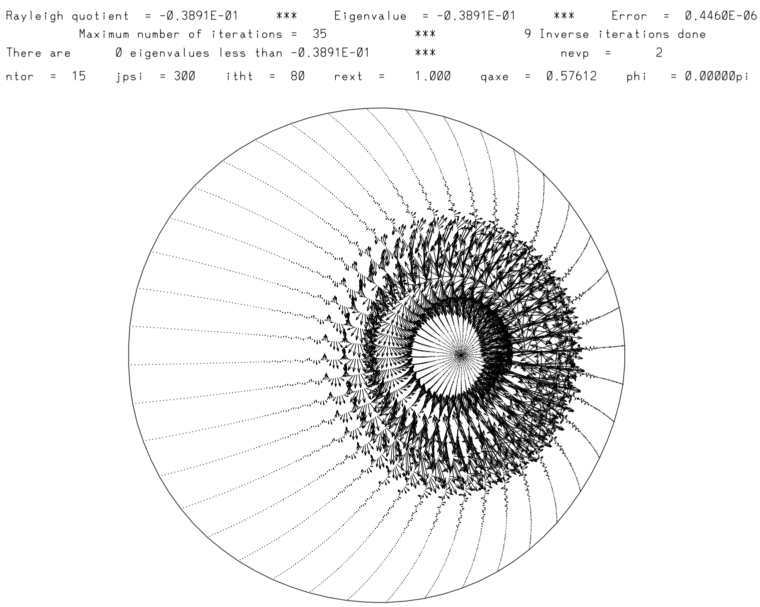

Lower harmonics

Fourier Analysis for imag Xpsi, chi = chi

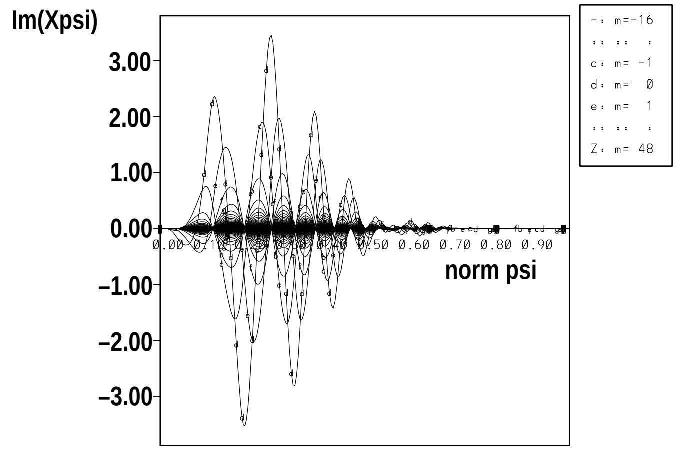

Without ballooning transformation

Finger like structure

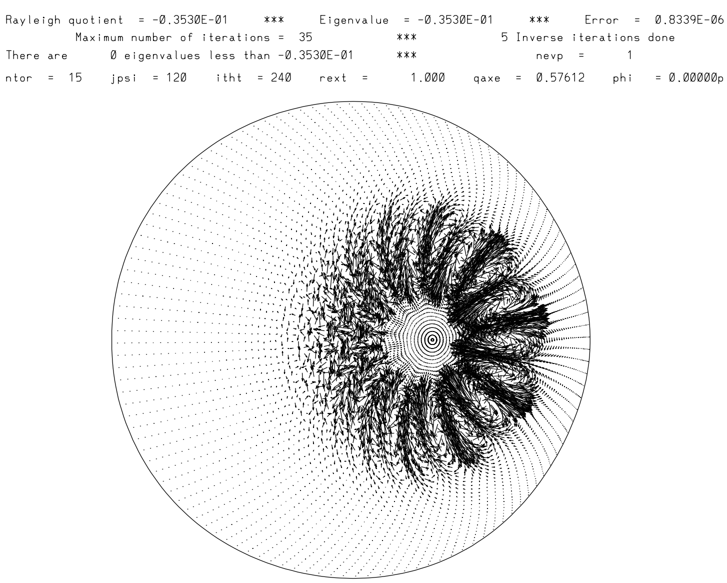

Higher harmonics

Fourier Analysis for imag Xpsi: pest = chi